Taylor & Francis
Taylor & Francis Group

ORIGINAL RESEARCH

◯ OPEN ACCESS ⓡ Check for updates

Immunotherapy with IL12 and PD1/CTLA4 inhibition is effective in advanced ovarian cancer and associates with reversal of myeloid cell-induced immunosuppression

Paul G. Pavicic Jr.[a], Patricia A. Rayman[a], Shadi Swaidani[a], Amit Rupani[a], Vladimir Makarov[a], Charles S. Tannenbaum[b], Robert P. Edwards[c], Anda M. Vlad[c], C. Marcela Diaz-Montero[a], and Haider Mahdi[c,d,e,f]#

[a]Center for Immunotherapy & Precision Immuno-Oncology (CITI), Lerner Research Institute, Cleveland Clinic, Cleveland, OH, USA; [b]Department of Inflammation and Immunity, Cleveland Clinic, Lerner Research Institute, Cleveland, OH, USA; [c]Department of Obstetrics, Gynecology and Reproductive Sciences and Magee Women's Research Institute, University of Pittsburgh School of Medicine, Pittsburgh, PA, USA; [d]Division of Gynecologic Oncology; Obstetrics, Gynecology and Women's Health Institute, Cleveland Clinic, Cleveland, OH, USA; [e]Translational Hematology Oncology Research Department, Taussig Cancer Institute, Cleveland Clinic, Cleveland, OH, USA; [f]Genomic Medicine Institute, Lerner Research Institute, Cleveland Clinic, Cleveland, OH, USA

ABSTRACT

The tumor microenvironment (TME) in ovarian cancer (OC) is characterized by immune suppression, due to an abundance of suppressive immune cells populations. To effectively enhance the activity of immune checkpoint inhibition (ICI), there is a need to identify agents that target these immunosuppressive networks while promoting the recruitment of effector T cells into the TME. To this end, we sought to investigate the effect of the immunomodulatory cytokine IL12 alone or in combination with dual-ICI (anti-PD1 + anti-CTLA4) on anti-tumor activity and survival, using the immunocompetent ID8-VEGF murine OC model. Detailed immunophenotyping of peripheral blood, ascites, and tumors revealed that durable treatment responses were associated with reversal of myeloid cell-induced immune suppression, which resulted in enhanced anti-tumor activity by T cells. Single cell transcriptomic analysis further demonstrated striking differences in the phenotype of myeloid cells from mice treated with IL12 in combination with dual-ICI. We also identified marked differences in treated mice that were in remission compared to those whose tumors progressed, further confirming a pivotal role for the modulation of myeloid cell function to allow for response to immunotherapy. These findings provide the scientific basis for the combination of IL12 and ICI to improve clinical response in OC.

Introduction

Ovarian cancer (OC) is the most lethal gynecologic cancer in the US.[1] Advanced stage OC has a five-year overall survival rate of 20–30% and more than 50% of patients that respond to current therapies experience recurrent disease.[2–4] Recurrent, platinum-resistant OC is characterized by only minimal responses to chemotherapy (<10–15%) and a poor prognosis, with overall survival estimated to be <12 months.[5–10] Thus, there is an urgent need to identify novel therapies to improve the outcomes of these patients. The impact of immunotherapy with immune checkpoint inhibitors (ICI) has been significant, providing durable response rates in several cancers. However, the response rates in ovarian cancer are low, ranging from 11% to 15% in platinum-resistant, recurrent settings.[11,12] Compared to nivolumab (anti-PD1) alone, dual immunotherapy with nivolumab and ipilimumab (anti-CTLA4) was associated with a higher objective response rate (31% vs. 12%) but with limited durability (3.9 vs. 2 months).[13] Therefore, it is critical to explore strategies with the potential to enhance the efficacy of

current PD1/PD-L1-based immunotherapy by targeting pathways that mediate resistance to ICI.

Myeloid cell subtypes with immunosuppressive functions, such as tumor associated macrophages (TAM) and myeloid-derived suppressor cells (MDSC) are frequently found infiltrating the tumor microenvironment (TME) of OC[14–18] and likely contribute to tumor progression, poor survival, and resistance to therapies including ICI.[14–18] MDSC can be divided into two phenotypically and functionally distinct subsets based on similarities to monocytes (M-MDSC) or neutrophils (PMN-MDSC). However, despite these differences, both subtypes are capable of suppressing the function of anti-tumor T cells.[19] We have previously shown that tumor-associated myeloid cells are prominent in the OC TME and correlate with poor survival and resistance to immune checkpoint inhibition.[18,19] Therefore, a potential strategy to modulate the tumor immune microenvironment to enhance the efficacy of immunotherapy in ovarian cancer is to target these

immunosuppressive cell types. IL12 is a strong modulator of dendritic cells, as it enhances their ability to polarize toward the Th1 responses crucial for effective tumor rejection.[20–22] IL12 was also reported to reprogram intratumoral MDSC in a preclinical melanoma model by reversing their suppressive role in vivo and enhancing cytotoxic T lymphocyte activity.[23] In addition to its effect on myeloid cells, IL12 also plays a central role in the activation of T and NK cells by promoting their proliferation and by enhancing the secretion of effector cytokines, such as IFNγ.[24] IL12 also has antitumor activity in IL12Rβ1-expressing tumors through IFNγ-mediated upregulation of MHC Class I molecules.[25]

Here, we tested the ability of IL12 to synergize with dual-ICI (anti-PD1+anti-CTLA4) in the preclinical ID8-VEGF immunocompetent murine model of advanced OC. Our results demonstrated that a combination of IL12 and dual-ICI resulted in enhanced durable anti-tumor activity and survival of mice bearing ID8-VEGF tumors as compared to those treated with monotherapy. Improved anti-tumor activity was associated with increased tumor infiltration by T cells and a downregulation of the phenotypic traits of myeloid cells known to mediate immunosuppression, leading to enhanced effector function of the infiltrating T cells. These results support the use of IL12 as a strategy to enhance the efficacy of dual PD1 and CTLA4 blockade in the treatment of OC.

Materials and methods

Mice and tumors

All experiments were performed under institutional animal care and use committee (IACUC) protocols adhering to USDA guidelines. Female C57BL6/J mice were purchased from The Jackson Laboratory (Bar Harbor, MA) and maintained pathogen-free under UDSA guidelines. Mice 6 to 8 weeks of age were used for subsequent studies. ID8-VEGF, an ovarian carcinoma cell line derived from spontaneous *in vitro* malignant transformation of C57BL/6 mouse ovarian surface epithelial cells and engineered to overexpress vascular endothelial growth factor (VEGF), as previously described,[26] was maintained in high glucose Dulbecco's Modified Eagle Medium (Sigma) supplemented with 4% Fetal Bovine Serum, 5 µg/mL insulin, 5 µg/mL transferrin, and 5 ng/mL sodium selenite (1× ITS; Sigma) and 1× Penicillin-Streptomycin solution in 5% CO_2 atmosphere at 37°C. These cells were obtained from Dr. Vincent Tuohy at the Cleveland Clinic.

Tumors were established by intraperitoneal (i.p.) injection of 5×10^6 ID8-VEGF tumor cells. As indicated, mice received 200 µg of anti-PD1 antibody (BioXcell, Clone RMP1–14) and/ or 200 µg of anti-CTLA4 antibody (BioXcell, Clone 9D9) via i. p. injection twice weekly, and/or 100 ng recombinant murine IL12p70 (IL12) (PeproTech) via i.p. injection three times a week. Weight gain due to ascites accumulation was used as a surrogate for tumor progression and mouse total body weight measurements were taken at 1–3 day intervals.

To investigate the impact of therapy on advanced disease, treatment was started 21 days after tumor implantation to ensure tumor establishment and onset of ascites accumulation prior to treatment. Tumor-bearing mice were randomized into four treatment groups – untreated control, IL12, anti-PD1 plus anti-CTLA4 with or without IL12. Animals were sacrificed at an established endpoint – either when total weight gain reached a 50% increase over baseline weight or when the mice presented symptoms of terminal illness. Animals in the control group and those treated only with immune checkpoint inhibition met endpoint at day 40. A subset of animals from treatment groups receiving IL12 were also harvested for analysis prior to endpoint at Day 35. Peritoneal tumor lesions, ascites, and peripheral blood were harvested for analysis.

RNA extraction and sequencing

ID8-VEGF whole-tumor lesion samples were dissected from the peritoneal cavity and immediately homogenized in TRI Reagent (Molecular Research Center, Inc. Cincinnati, OH) using a Tissue-Tearor handheld mechanical homogenizer (BioSpec Products, Inc. Bartlesville, OK.). Ascites samples were collected from the peritoneum of mice, and CD11b+ cells were purified utilizing MACS MicroBead column-based magnetic cell isolation system (Miltenyi Biotec.). Briefly, a portion of viable cells obtained from ascites were labeled with anti-CD11b-PE antibody followed by incubation with anti-PE MACS magnetic microbeads. CD11b+ cells were captured by passing antibody- and microbead-conjugated cells through a MACS separation column in the presence of a magnetic field and eluted by washing the column outside of the magnetic field. Total RNA was isolated from samples in TRI reagent according to manufacturer's instruction, and the RNA concentration was measured using NanoDrop ND-1000. Libraries were prepared using the Illumina TruSeq stranded mRNA kit and sequenced at 80 M reads (40 M paired ends) on a NovaSeq Sequencing System from Illumina.

Bioinformatics

Raw reads in the FASTQ format were aligned to mm10 reference genome using the STAR aligner.[27] The feature "Counts read summarization program"[28] was used to count mapped reads for each gene in the mm10 annotation file (gencode. vM25.annotation.gtf). Count files were then merged by an in-house R script and normalized using DESeq2.[29] DESeq2 standard differential gene expression analysis was used to compare two groups at a time for GSEA. For hierarchical clustering, a Likelihood Ratio Test was run in DESeq2, and clustering was performed using the Pheatmap R package on the top 200 most significant (lowest adjusted *p* value) differentially expressed genes.

Cytokine analysis

Quantification of cytokines present in the ascites fluid from mice bearing ID8-VEGF tumors was performed using the Meso Scale Discovery Multi-Spot Assay System (Meso Scale Diagnostics, LLC). V-PLEX assays were performed using Cytokine Panel 1, Proinflammatory Panel 1, and Th17 Panel 1 mouse kits, as well as a TGF-B kit, per manufacturer's instructions. Briefly, MULTI-SPOT assay plates pre-coated with capture antibodies were washed and incubated with

diluted ascites fluid samples and/or calibrators for 2 h at room temperature. Next, plates were washed and bound analytes measured using detection antibodies conjugated with electro-chemiluminescent labels (MSD SULFO-TAG). Following an additional 2-h incubation at room temperature, plates were washed, incubated with electrochemiluminescence buffer, and analyzed on a MESO QuickPlex SQ 120 instrument. Data was processed using the MSD Discovery Workbench Version 4.0.

FACS and antibodies

Viable cells derived from blood and ascites from ID8-VEGF tumor-bearing mice were assessed for the frequency of T cell and myeloid cell subsets. Cell suspensions were stained with antibodies for CD45 (Clone 30-F11), T cell markers – CD4 (Clone GK1.5), CD8 (Clone 53–6.7), CD127 (Clone SB/199), CD25 (Clone *M*- A251) and PD1/CD279 (Clone J43) or myeloid markers – Ly6G (Clone RB6-8C5), CD11b (Clone M1/70), CXCR2 (Clone V48–2310), CD11c (Clone HL3), CCR2 (Clone 475,301), F4/80 (Clone T45–2342), I-A/I-E (clone M5/114.15.2, BioLegend), or PDL1/CD274 (Clone MIH5, eBioscience). Myeloid derived suppressive cells were gated as M-MDSC CD11b+Ly6Glo and PMN-MDSC CD11b+Ly6Ghi, dendritic cells as CD11b+CD11c +I-A/I-E+ and macrophages as CD11b+ F4/80+I-A/I-E+. Antibodies were from BD Biosciences unless otherwise specified. The cells were acquired for flow cytometry using the BD FACSymphony A5 cell analyzer, and data was subsequently analyzed with the FlowJo software package (BD Biosciences) using the plugins UMAP, XShift, and Cluster Explorer.

Single cell RNA sequencing

Cells isolated from peritoneal lavages of i.p. ID8-VEGF tumor-bearing mice that were in relapse or remission following intervention with dual-ICI + IL12 were subjected to single-cell RNA sequencing. Single-cell suspensions were prepared, loaded on the 10× Genomics Chromium System (Single Cell 3' v3 platform) and libraries prepared according to manufacturer's specifications. The concentration and quality of double-stranded cDNA was assessed using a high-sensitivity DNA assay on an Agilent 2100 Bioanalyzer. Library preparation for sequencing on an Illumina platform was accomplished for each sample following the manufacturer's protocol (10× Genomics, CG000183 Rev A). The quality of library construction was again assessed using the Agilent 2100 Bioanalyzer. Samples were first fluorometrically quantified with a Qubit fluorometer (Thermo Fisher Scientific), pooled, and again quantified on a Quantabio Q cycler using the Quantabio SparQ Fast Library Quant kit. Sequence data was generated on a NovaSeq 6000 using parameters recommended by the manufacturer (10× Genomics, CG000183 Rev A). The bioinformatics of output data was performed using Cell Ranger software (10× Genomics) mkfastq, count, and AGGR functions. Subsequently, Cell Loupe browser (10× Genomics) files were generated, and data visualized by UMAP, individual gene, and heat map plots.

Statistical analyses

For each experiment, five animals per group were planned and expected to yield a power of 80% to detect statistically significant differences between experimental groups. P-values were calculated using Student's *t*- test and a significant difference was defined as a $P < 0.05$. The overall survival was calculated using a Kaplan–Meier curve.

Results

Combinatory treatment with IL12 and dual-ICI results in sustained anti-tumor activity in a preclinical model of advanced ovarian cancer

For our studies, we utilized the ID8-VEGF cell line, a widely adopted, aggressive preclinical murine model of ovarian cancer. When implanted in the peritoneum of immunocompetent mice, this model mimics the characteristics of human ovarian cancer by rapidly developing peritoneal tumor lesions and ascites within 20 days, with the experimental endpoint being generally achieved by approximately day 40. Tumor burden was assessed by measuring weight gain due to ascites accumulation. To mimic advanced stage intervention, treatment commenced 21 days after peritoneal ID8-VEGF implantation [Figure 1A]. Mice were treated with dual-ICI (anti-PD1 and anti-CTLA4 antibodies), IL12, or combination dual-ICI + IL12. Mice responded to IL12 alone, and to an even greater extent if they received a combination dual-ICI + IL12 [Figure 1B]. Animals treated with IL12 alone showed reduced weight gain by five days of treatment compared to the untreated group, but continued to progress during the course of treatment. Interestingly, the mice in the dual-ICI + IL12 arm did not respond until after 14 days of treatment but showed up to a 41% reduction of weight gain by 9 days after completion of the regimen. While dual-ICI therapy did not impact median survival when administered alone, IL12 monotherapy increased mouse survival by 11.5 days. Survival was further extended by co-treatment with IL12 and dual-ICI (19.5 days compared to untreated mice) [Figure 1C]. Both the IL12 and IL12 + dual-ICI were associated with lower frequency of tumor (CD45^{neg}) cells within the ascites. [Figure 1D]. The synergistic effect of IL12 and dual-ICI was also observed, although to a lesser extent, in the early-stage setting in which treatment started 4 days following ID8-VEGF implantation [Supplemental Figure S1]. These results suggest that immunomodulation by IL12 results in a transient antitumor effect in the advanced stage setting of the ID8-VEGF ovarian cancer model, which can be further potentiated to longer term response and survival by the addition of PD1 and CTLA4 blockade.

IL12 alters the composition of circulating immune cell types in mice bearing ID8-VEGF

We performed a high parameter flow cytometry analyses of blood samples collected from tumor-bearing mice after 15 days of treatment. Notable changes in the frequencies of circulating immune cell types were observed after the administration of IL12 alone or in combination with dual-ICI [Figure 2A].
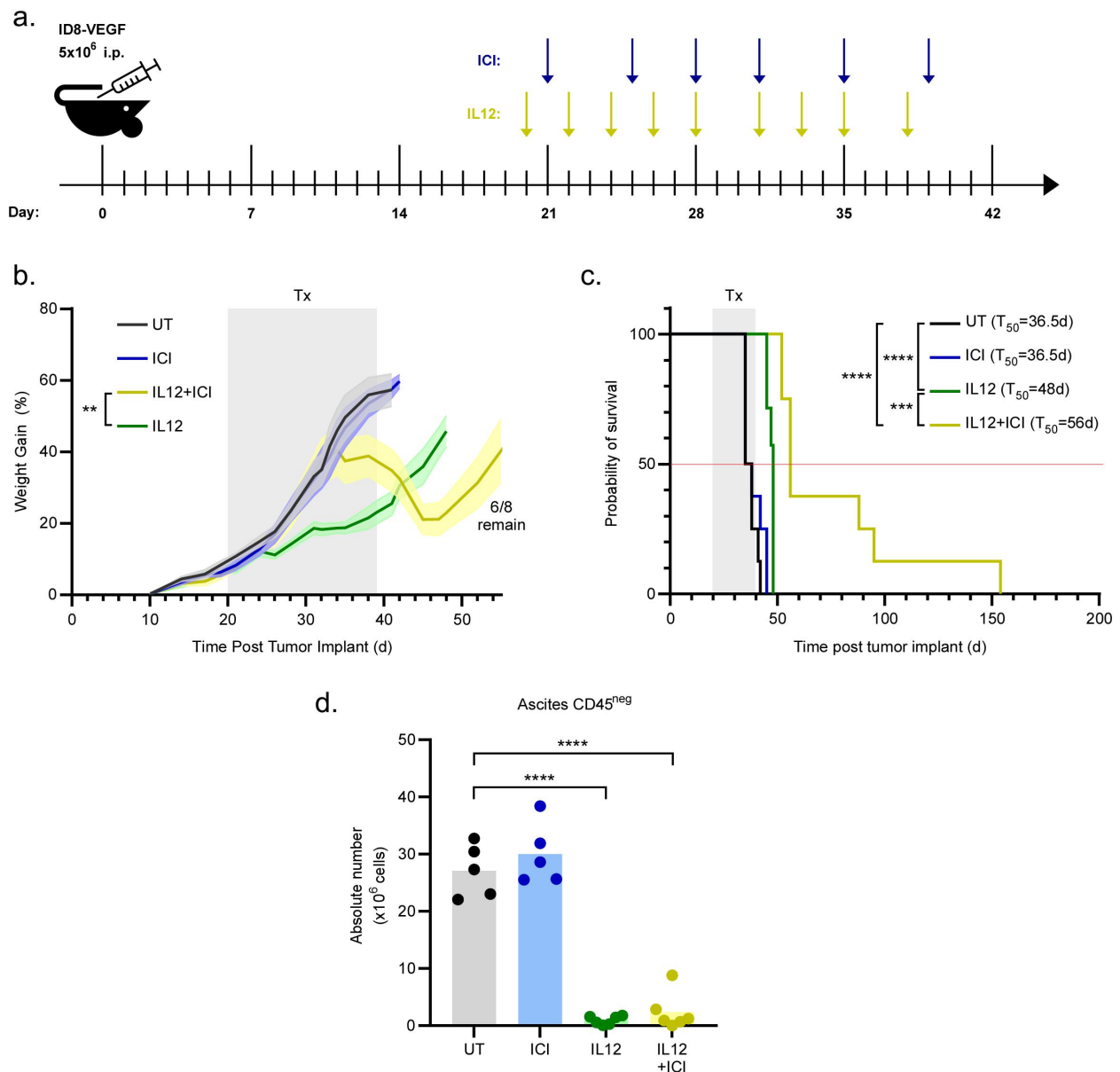
Figure 1. Combination treatment of IL12 with dual-ICI results in enhanced durability of response in the ID8-VEGF advanced ovarian cancer preclinical tumor model. Female C57BL/6 mice were injected intraperitoneally with 5×10^6 ID8-VEGF tumor cells, randomized into treatment cohorts ($n = 7$ or 8 for each group), and evaluated daily for clinical signs of disease progression. (a) treatment schema was designed to mimic intervention at advanced stage disease. Recombinant murine IL12 with or without immune checkpoint monoclonal antibodies were administered via intraperitoneal injection starting at day 20 as described in *materials and methods*. Arrows represent days which mice received indicated intervention. (b) weight gain due to abdominal accumulation of ascites was used as proxy of tumor progression and measured at regular intervals. Response to treatment with IL12 alone or with anti-PD1 + anti-CTLA4 monoclonal antibodies, was monitored by changes in weight gain. (c) overall survival was tabulated based on time taken for animals with progressing disease to reach humane endpoint and survival was calculated using Kaplan-Meier analysis with statistical significance evaluated by log-rank (Mantel-Cox) test. (d) a subset of mice from each treatment group was sacrificed 35 days following ID8-VEGF tumor implantation. The total volume of ascites fluid was collected from the abdomen and subjected to flow cytometry to measure the total number of tumor cells (CD45neg) within the abdominal cavity. *P* values were calculated using student's t-test. Statistically significant differences between indicated treatment groups were marked with asterisks (*p < 0.05, ***p < 0.005, ****p < .001).

Within the myeloid compartment, the administration of IL12, irrespective of dual-ICI, increased the levels of circulating MDSC [Figure 2B]. Numbers of monocytic MDSC (M-MDSC) went up 2.9-fold with IL12 treatment alone and 2.2-fold when combined with dual-ICI. Polymorphonuclear MDSC (PMN-MDSC) were less abundant compared to M-MDSC but were also upregulated in response to IL12 therapy: there was a 3.1-fold change with IL12 alone and a 4.7-fold change when combined with dual-ICI. Further, treatment differentially impacted PDL1 expression on MDSC subsets: - in

the untreated setting, 53.5% of circulating M-MDSC expressed PDL1 as compared to 8.6% of PMN-MDSC. The frequency of circulating PDL1+ PMN-MDSC increased from 8.6% without treatment to 64.2% with IL12 alone, and to 83.5% with IL12 + dual-ICI. M-MDSC were less affected by treatment, as we found that circulating PDL1+ M-MDSC decreased significantly by 11.2% but increased by 19.5% in groups treated with IL12 or IL12 plus dual-ICI, respectively, as compared to the untreated animals. Further, treatment with IL12 correlated with a 13.1-fold increase of the number of macrophages and
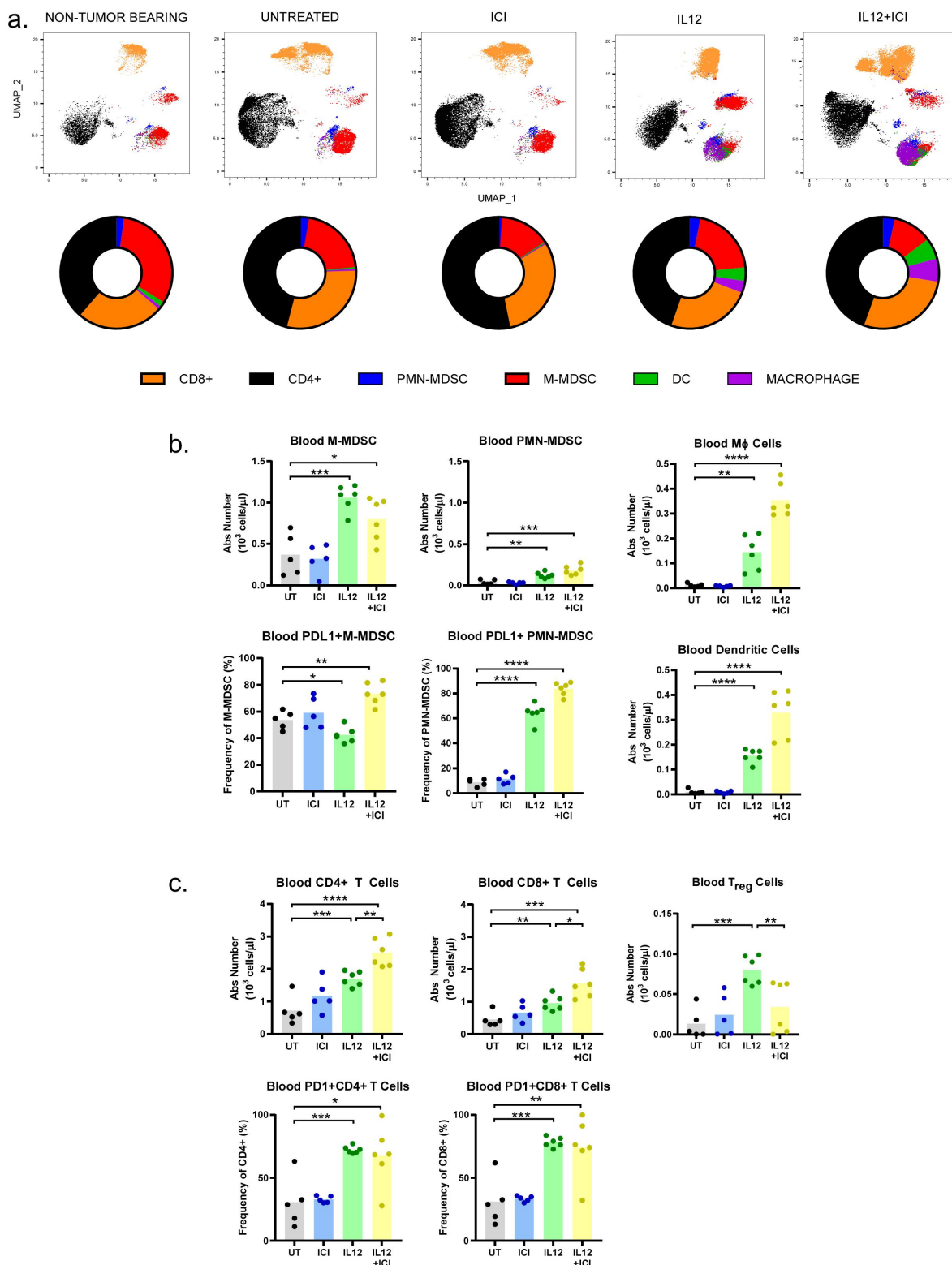
Figure 2. IL12 and checkpoint inhibition alter the composition of circulating immune cell types in mice bearing ID8-VEGF tumors. (a) High parameter flow cytometry was used to assess the cellular composition of blood from mice 35 days after tumor implantation using antibody panels described in *materials and methods*. (b) absolute numbers of monocytic and polymorphonuclear MDSC, macrophage, and dendritic cells were determined. Further, frequency of MDSC subsets that expressed PDL1 were calculated. (c) absolute numbers of CD4+, CD8+, and T_{reg} T lymphocytes were delineated. The frequency of CD4+ and CD8+ T cells that expressed PD1 was also measured. Each dot represents measurement from an individual mouse, $n = 5$ or 6 for each group. *P* values were calculated using Student's t-test. Statistically significant differences between indicated treatment groups were marked with asterisks (*p < 0.05, ***p < 0.005, ****p < .001).

a 16.3-fold increase in dendritic cells in the periphery; when combined with dual-ICI this effect was enhanced 2.5 and 2.1 times, respectively. Increases in the numbers of circulating T lymphocyte populations in response to IL12 treatment were observed – CD4+ T cells increased 2.4-fold and CD8+ T cells 2.1-fold [Figure 2C]. The combination treatment mildly amplified this effect in both populations 1.5 times. In contrast, significant induction of PD1 expression was noted on both CD4+ and CD8+ T cells after treatment with IL12 alone or in combination with dual-ICI. An increase in the frequency of T regulatory cells (T_{reg}) was observed after treatment of IL12 alone, however this effect was abrogated in mice treated with a combination of IL12 and dual-ICI. Altogether, these results suggest that IL12, alone or in combination with dual-ICI, not only induces changes in the frequencies of circulating immune cells – both myeloid and lymphoid – but also increases the expression of regulatory molecules, such as PDL1 on PMN-MDSC and PD1 on T cells. The increase in the frequency of T_{reg} mediated by IL12 alone can partly explain the role of anti-CTLA4 in enhancing the anti-tumor immune response when IL12 was combined with dual-ICI.

IL12 in combination with dual-ICI polarizes the immune landscape toward an anti-tumor response

To better understand the mechanisms behind the synergistic effect of IL12 and dual-ICI, we performed comprehensive immunophenotyping of the tumor microenvironment (TME) by analyzing both ascites and peritoneal tumor lesions. High parameter flow cytometry analyses of ascites revealed changes in the overall immune landscape in response to immunotherapy [Figure 3A]. Within the myeloid compartment, IL12 administration alone resulted in a 75-fold decrease in the numbers of M-MDSC in the ascites, and when IL12 therapy was combined with dual-ICI they were nearly ablated [Figure 3B]. As noted in the blood, there were fewer PMN-MDSC in the ascites compared to M-MDSC, and treatment did not significantly impact the numbers of PMN-MDSC. The frequency of M-MDSC expressing PDL1 rose from 11.0% in untreated mice to 83.5% with IL12 treatment and to 98.3% after combination therapy with IL12 and dual-ICI. In untreated mice, a larger proportion of PMN-MDSC were PDL1+ compared to M-MDSC, 86.8% vs 11.0%, which was enhanced to 97.5% with IL12 alone and 99.7 with IL12 + dual-ICI. We noted a reduction in the numbers of ascites derived macrophages in response to treatment – IL12 monotherapy associated with a 1.9-fold depletion of macrophages, which was further reduced to a 3.3-fold depletion when combined with dual-ICI. These data suggest that IL12 plays a significant role in modulating the M-MDSC, which are prominent immunosuppressive cells in the ascites.

A significant decrease in the levels of dendritic cells, described here as MHCII+ CD11b+CD11c+, was observed in mice treated with IL12 alone (8.9-fold change) or in combination with dual-ICI (56.1-fold change) which could be related to the mobilization of these cells to within tumor tissue/implants. The number of T lymphocytes in the ascites was not significantly altered in response to therapy, possibly due to increased homing of these cells to tumor lesions. However, the status of PD1 expression on both CD4+ and CD8+ T cell subsets was significantly increased, indicating activation of these cells [Figure 3C]. As observed in the blood, when treated with IL12, the frequency of CD4+, and CD8+ T cells in the ascites that expressed PD1 increased 4.0 and 5.7-fold, respectively, compared to those from untreated mice. The addition of dual-ICI to IL12 did not impact this effect, but the synergistic effect on tumor progression may be explained by the reversal of T cell exhaustion following IL12 activation of T cells.

We further profiled the tumor inflammation by measuring several cytokines in the ascites, using the Meso Scale Discovery Multi-Spot Assay System. Dual-ICI alone had minimal effect on secretion of cytokines in the ascites; however, treatment with IL12 was associated with significant accumulation of inflammatory cytokines, including those involved in the effector activity of T cells [Figure 3D]. Levels of IFNγ were enhanced by IL12 (>4000-fold) but did not significantly change with combination therapy. Effector cytokines such as IL2, IL4, and IL21 as well as inflammatory cytokines such as IL1β, IL5, IL6, IL27, TNFα, and MIP1α were associated with enhanced levels (>5-fold) in ascites from mice treated with combination therapy compared to IL12 alone. Compared to levels in the ascites from untreated mice, IL12 monotherapy stimulated a 50-fold increase in IL12p70 production though, interestingly, with combination therapy the increase was 10-fold less.

Next, we performed bulk transcriptomic analysis using RNA isolated from ID8-VEGF tumor tissue of mice treated or not with the combinations of IL12 and dual-ICI [Figure 4]. Hierarchical clustering of samples by the top 500 variable genes showed distinct expression patterns among treatment groups [Figure 4A]. A correlation between median survival and gene expression was observed as evidenced by overlap in hierarchical clustering of samples from replicate untreated mice and those treated with dual-ICI monotherapy (lowest median survival) but distinct from samples from mice treated with IL12 alone and IL12 with dual-ICI (higher median survival) where the expression pattern was well defined. Cell type analysis was performed using xCell, a gene signature-based method to infer immune and stromal cell types within the tumor [Figure 4B]. Compared to other treatment groups, IL12 + dual-ICI associated with elevation of several cell types including B cells, T cells, monocytes, macrophages, and dendritic cells. These data further support that there is increased infiltration and recruitment of these cells and mobilization from blood and ascites to the TME of OC tumors. Interestingly, cell types such as mesenchymal and hematopoietic stem cells as well as endothelial cells were reduced in tumors treated with combinatory therapy consistent with other anti-tumor effects mediated by IL12. The top 50 genes differentially expressed in tumors treated with IL12 + dual-ICI versus those left untreated included T cell effector genes and genes that promote inflammatory genes such as CCL5, CCL19, CXCL9, CXCR6, GZMB, GZMK, IFNG, IL21, and NKG7 [Figure 4C]. Further, Gene Set Enrichment analysis (GSEA) was performed in order to discern the associated cancer hallmarks between treatment groups. We found that gene signatures involved in immune related pathways – IL6 JAK STAT3 signaling, allograft rejection, TNFα signaling via NFκB, inflammatory response, and interferon alpha and gamma response – associated with
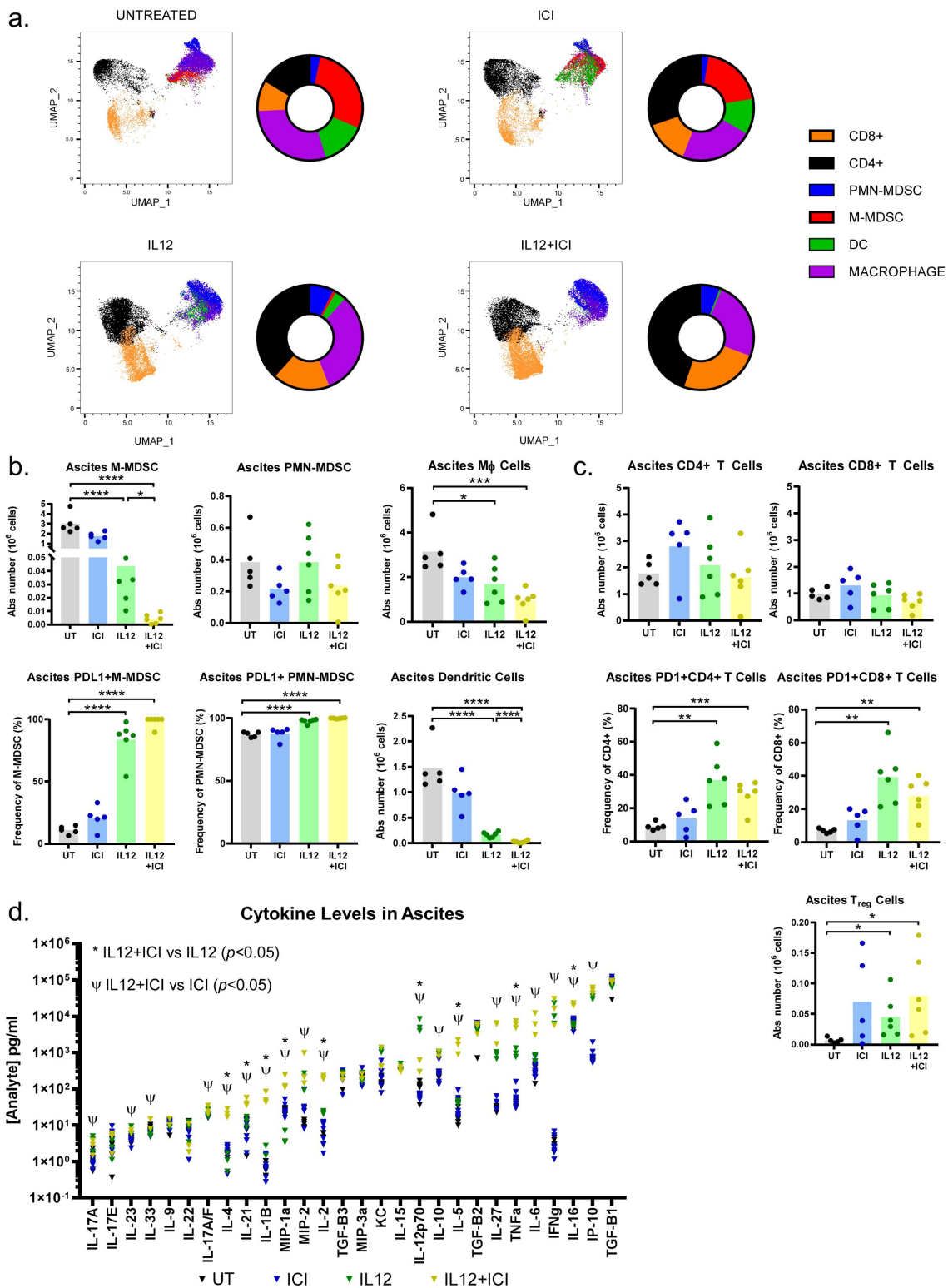
Figure 3. IL12 in combination with checkpoint blockade conditions the immune landscape toward an anti-tumor response in mice bearing ID8-VEGF tumors. (a) high parameter flow cytometry was used to assess the cellular composition of ascites from mice 35 days after tumor implantation using antibody panels described in *materials and methods*. (b) absolute numbers of monocytic and polymorphonuclear MDSC, macrophage, and dendritic cells were determined and frequency of mdsc subsets that expressed pdl1 were calculated. (c) absolute numbers of CD4+, CD8+, and T_{reg} T lymphocytes were measured and the frequency of CD4+ and CD8+ T cells that expressed PD1 was also determined. Each symbol represents measurement from an individual mouse, $n = 5$ or 6 for each group. P values were calculated using Student's t-test. Statistically significant differences between indicated treatment groups were marked with asterisks (*$p < 0.05$, ***$p < 0.005$, ****$p < 0.001$). d cytokine levels were measured using meso scale discovery multi-spot assay system kits including Cytokine Panel 1, Proinflammatory Panel 1, Th17 Panel 1 and TGF-B kits. Individual cytokines that had statistically significant differences ($p < 0.05$) comparing combinatory treatment vs IL12 monotherapy were marked with an asterisk. Statistically significant differences ($p < 0.05$) comparing combination vs IL12 alone were indicated with Ψ.
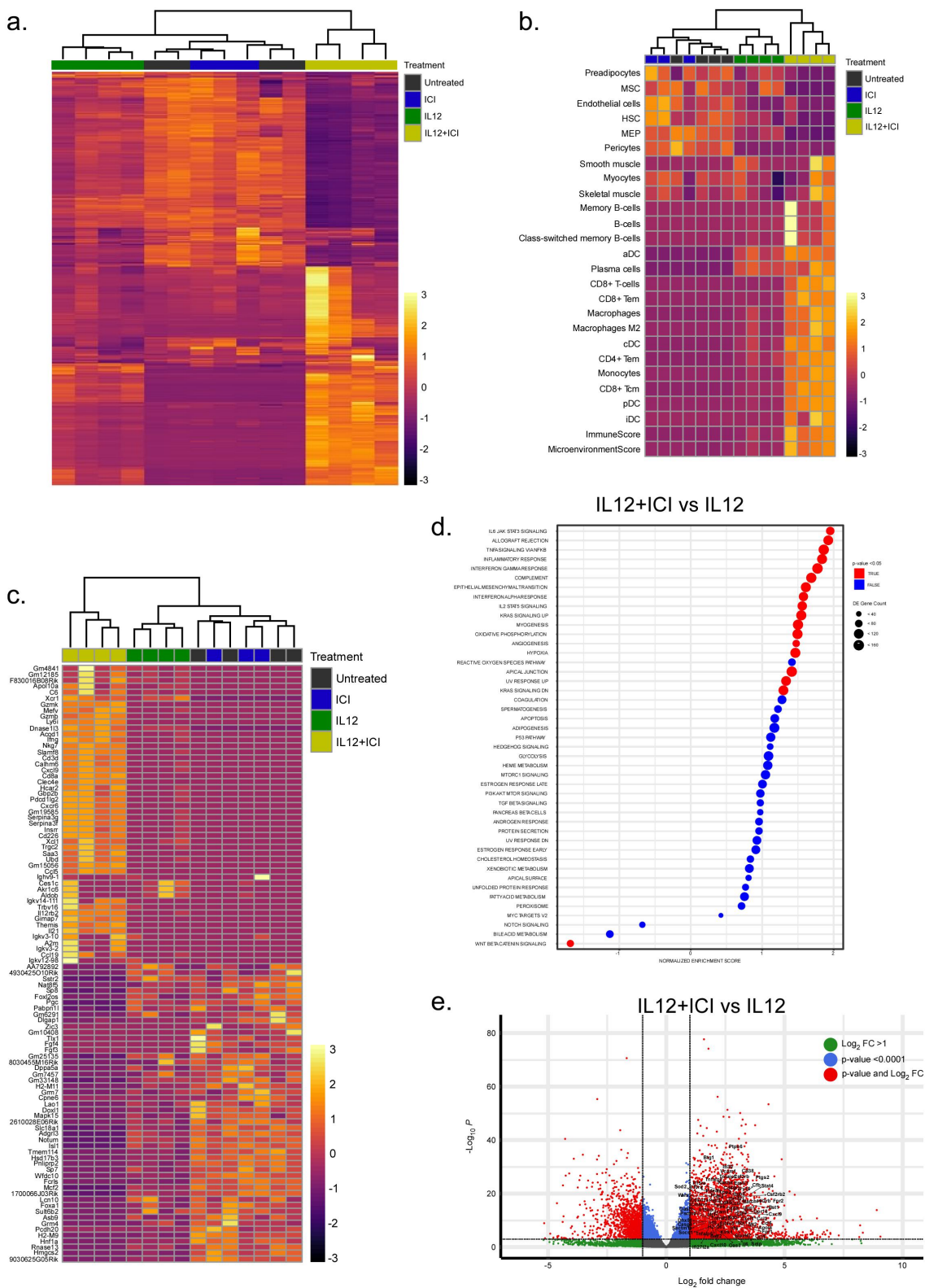
Figure 4. Treatment with IL12 and dual-ICI associates with distinct patterns of gene expression in solid lesions from peritoneum of mice bearing ID8-VEGF tumors. Bulk RNA sequencing of ID8-VEGF solid tumor lesions. For heat maps, each column represents individual mice and the treatment group is indicated by color code at top. (a) heat map with hierarchical clustering based top 500 variable genes. (b) cell type enrichment analysis based on gene expression data using *xCell*. (c) heat map with hierarchical clustering of top 50 differentially expressed genes in tumors from untreated versus IL12+dual-ICI. (d) hallmarks of cancer gene set enrichment analysis. Gene sets with statistically significant changes in expression comparing IL12+dual-ICI vs IL12 alone are indicated with red colors and the size of the dot is representative of the number of genes in the corresponding gene set that are significantly changed. (e) volcano plot of differentially expressed genes in ID8-VEGF tumors from mice treated with IL12 alone versus IL12+dual-ICI. Fold change and significance cutoffs are as indicated and named genes are members of the hallmarks of cancer *Interferon Gamma Response* gene set that were significantly upregulated by at least three-fold.

a significant enhancement in lesions from mice treated with IL12+dual-ICI versus IL12 alone [Figure 4D]. Interestingly, Wnt beta catenin signaling showed a negative association with IL12+dual-ICI treatment. Genes differentially expressed in tumor lesions treated with IL12 with or without dual-ICI were compared using a volcano plot to visualize the magnitude of statistically significant changes [Figure 4E]. Seventy-four genes designated as prototypic members of the Interferon Gamma Response gene set were significantly upregulated by at least three-fold. This suggests that the extended survival achieved by combination therapy as compared to IL12 treatment alone might be attributable to the effect the dual treatment has on primarily modulating the interferon gamma pathway with its subsequent effect.

Long-term responses after IL12 and dual-ICI treatment associate with reversal of immunosuppression by myeloid cells

To better understand the contribution that myeloid function has on the anti-tumor responses induced by IL12 in combination with dual-ICI, we extracted RNA from purified CD11b+ cells in ascites and performed bulk transcriptomic analyses [Figure 5A]. Hierarchical clustering of the top 50 upregulated and downregulated genes in ascites CD11b+ cells bifurcated into one of two groups, depending on whether treatment also included IL12 in addition to the dual-ICI [Figure 5A]. Further, the unique clustering of samples also highlighted the impact of dual-ICI on myeloid gene expression. Gene set enrichment analysis was also carried out to investigate the impact of IL12 therapy, with or without dual-ICI, on cancer hallmarks in the myeloid compartment of the TME. Several inflammatory pathways were activated in CD11b+ cells from the ascites of mice treated with IL12 + dual-ICI as compared to IL12 alone [Figure 5B]. The interferon alpha response, interferon gamma response, allograft rejection, IL6 Jak STAT3 signaling, inflammatory response, IL2 STAT5 signaling, and TNFA signaling via NFKB all showed positive normalized enrichment scores. Negative associations were noted for prototypic pathways involved in development and metabolic processes including epithelial mesenchymal transition, myogenesis, heme metabolism, and cholesterol homeostasis. Further, 54 inflammation-related genes designated as cancer hallmarks were differentially expressed at least two-fold in CD11b+ cells from the ascites of mice treated with IL12+dual-ICI versus IL12 alone and are named in the volcano plot in Figure 5C. The direct effect of IFNγ was corroborated by the in vitro culture of CD11b cells isolated from ascites of untreated mice. An increase in the expression of pro-immune mediators, such as CXCL9, CXCL10, CXCL11 and β2-microglobulin was observed after the in vitro culture with IFNγ [Supplemental Figure S2].

Single cell transcriptomics defines distinct gene expression patterns of peritoneal cells during relapse or remission following dual-ICI treatment combined with IL12

We next compared the single-cell transcriptome of cells recovered from the peritoneum of mice that progressed with those from mice that remained in remission following treatment with IL12 and dual-ICI. Unbiased characterization of the transcriptional state of 7,674 and 7,006 cells recovered by peritoneal lavage from mice in relapse or remission, respectively, showed distinct UMAP-based clustering [Figure 6A]. Cell types were categorized based on the expression of marker genes and groups defined by K-means quantitative statistical clustering. Tumor cells, identified by a lack of expression of CD45 and elevated levels of Krt7, were only found in mice with active disease. Conversely, mice in remission had more peritoneal lymphocytes (mainly B cells and T cells) that express Cd45 and Cd2. Myeloid populations were found in both remission and relapsed settings; however, they represented two distinct clusters indicative of differential functional states [Figure 6B]. Enhanced expression of CCR2 ligands – CCL2, CCL7, CCL8, and CCL12 in myeloid (CD11b+) cells was associated with relapse. By contrast, fewer cells expressing CCR2 were present in the peritoneum of mice in remission. It is noteworthy that CCL2 is also produced by ID8-VEGF tumor cells themselves [Figure 6B] and may contribute to the initial recruitment of immunosuppressive myeloid cells to the TME. These infiltrating immunosuppressive myeloid cells can then perpetuate recruitment along with expression of other CCR2-directed chemokines. Furthermore, myeloid cells from mice in relapse demonstrated elevated expression of a collection of genes involved in immunosuppression and downregulation of genes associated with anti-tumor activity [Figure 6D]. These results suggest a crucial contribution of myeloid cells to the overall immune landscape of the OC tumor milieu and underscores the importance of targeting these cell types as a strategy to enhance the clinical benefit of immunotherapy.

Discussion

In this study, we demonstrate that IL12 in combination with dual-ICI resulted in superior anti-tumor activity with durable responses in the setting of an aggressive murine model of advanced stage ovarian cancer. We show that the combined regimen significantly increases the infiltration (as shown by transcriptomic data) and functional activation of T cells, resulting in elevated levels of IFNγ, which in turn counteracts the function of immunosuppressive myeloid cells. Such modulation of myeloid function resulted in an immune-promoting phenotype characterized by elevated expression of mediators involved in antigen presentation and recruitment of T cells into the TME. Proinflammatory myeloid factors, such as IL1β and TNFα, also significantly increased when IL12 was combined with dual-ICI therapy. IL12 is a potent immunomodulatory cytokine that has been shown to enhance the activity of CD8+ T cells by significantly enhancing the secretion of IFNγ.[30] Further, IL12 has a positive synergistic proliferative effect on pre-activated NK and T cells and also enhances their cytolytic capacity either independently and/or synergistically.[21,24,31] Ribas et al. showed that T cell infiltration and an IFNγ signaling signature were associated with increased likelihood of response to immune checkpoint therapy.[32]

Although our study only involved the use of a single preclinical model, it happens to be a universally accepted representation of human ovarian cancer and has been used in multiple studies aimed at understanding the potential role of
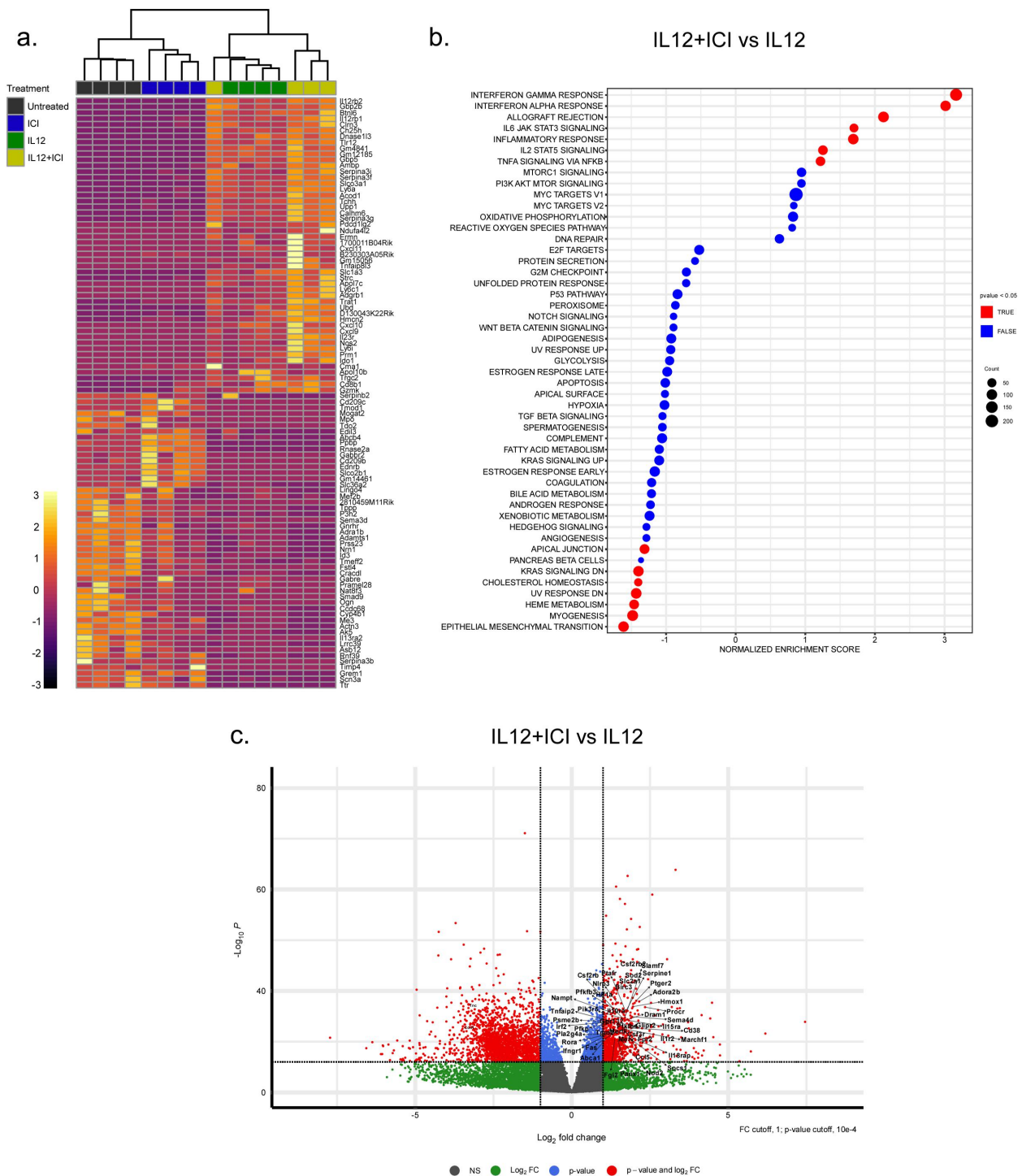
Figure 5. Combinatory therapy with IL12 and dual-ICI correlates with enhanced expression of genes related to inflammation in myeloid cells within the ascites. CD11b+ cells were isolated from the peritoneal cavity of tumor bearing mice and bulk RNA sequencing was performed. (a) heat map with hierarchical clustering based on top 50 differentially expressed genes comparing IL12+dual-ICI versus untreated animals. Each column represents individual mice and the treatment group is indicated by color code at top. (b) hallmarks of cancer gene set enrichment analysis comparing combination therapy vs IL12 alone. Gene sets with statistically significant changes in expression are indicated with red colors and the size of the dot is representative of the number of genes in the corresponding gene set that are significantly changed. (c) volcano plot of differentially expressed genes in peritoneal CD11b+ from mice treated with IL12+dual-ICI versus IL12 alone. Fold change and significance cutoffs are as indicated and named genes are inflammation-related hallmarks of cancer.

immunotherapy in ovarian cancer.[26] Importantly, our in vivo studies involved the intraperitoneal implantation of tumor cells as opposed to establishing flank tumors subcutaneously. This strategy allowed us to replicate the natural milieu and progression of ovarian cancer, characterized by the seeding of the peritoneal surfaces with tumor cells as well as the production of ascites. The ID8-VEGF OC model secretes high levels of VEGF (a therapeutic target of bevacizumab, widely used in ovarian cancer) and is more aggressive than the parental ID8 OC model.[33] In addition to being pro-tumorigenic, VEGF plays an important role in providing an immunosuppressive tumor microenvironment mediated by MDSC and other
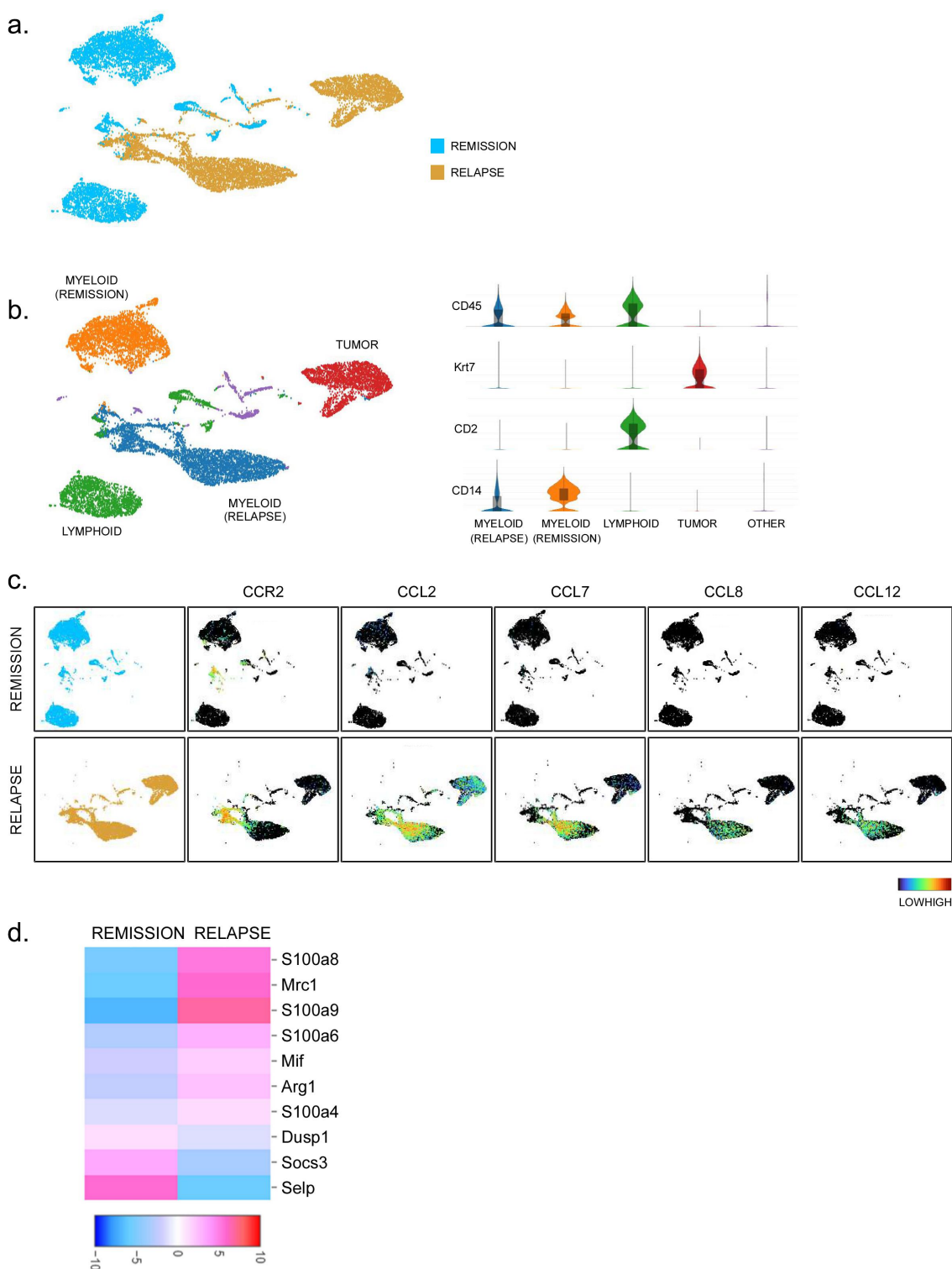
Figure 6. Single-cell RNA sequencing reveals distinct gene expression patterns of peritoneal cells isolated from ID8-VEGF tumor bearing mice in remission or relapse following local IL12 treatment with dual-ICI. (a) UMAP projection showing distinct clustering of peritoneal cells from mice in remission (blue) or relapse (gold) following treatment with IL12 + dual-ICI. (b) Color coded K means clustering and expression of cell markers CD45, *Krt7* (tumor), *Cd2* (lymphoid), and *Cd14* (myeloid) showing differential immune status within the peritoneum. Each point is color-coded by its cluster assignment and cell type. Violin plots show relative expression of marker genes between clusters. (c) UMAP projection, split based on remission (top row) or relapse (bottom row) disease status showing peritoneal cells expressing CCR2 and those expressing CCR2- directed chemokines CCL2, CCL7, CCL8, and CCL12. Each point is color coded based on expression level of the indicated genes from low (black) to high (red). (d) Heat map comparing level of expression of noted immunosuppressive genes in myeloid designated clusters of peritoneal cells from mice in relapse or remission following dual-ICI + IL12 therapy.

factors. Further, by starting treatment after 21 days of implantation we mimicked advanced disease, which represents a stage with few therapeutic options. Finally, the availability of both ascites and peritoneal tumor lesions allowed us to interrogate the changes in stromal components in response to therapy in a realistic TME context.

Our results are in agreement with the notion that ovarian cancer is characterized by an immunosuppressive TME. Therapy with ICI alone administered to hosts with established tumors, to mimic an advanced stage setting, did not have a significant effect on altering the TME, which could explain the only modestly elevated T cell activity and lack of response durability observed following ICI treatment in clinical trials.[11–13] Tumor-associated myeloid cells are prominent in ovarian cancer TMEs and have been shown to negatively impact CD8+ T cell responses, and to recruit T regulatory cells that promote an immunosuppressive TME and tumor progression.[16,17,34] We observed strong modulation of the levels and function of myeloid cells in response to IL12 treatment and to a greater extent when combined with dual-ICI. Circulating levels of M-MDSC increased in response to IL12 with or without dual-ICI treatment, though levels were lowered in the ascites to an almost undetectable level in mice treated with a combination of IL12 and dual-ICI. The significant decrease in M-MDSC in the ascites could be explained by their mobilization to the systemic circulation and/or alteration in their phenotype with changed into anti-tumorigenic myeloid cells. Furthermore, IL12 induced drastic changes in the expression of PDL1 among circulating PMN-MDSC and in M-MDSC in the ascites, supporting the need for anti-PD1/PDL1 blockade. Such a strong decrease of myeloid function within the ascites resulted in a pro-immune phenotype as evidenced by the accumulation of inflammatory mediators that favor effector anti-tumor responses (such as IL2, TNFα, and IL1β). These enhanced effector anti-tumor responses mediated durable responses and substantial tumor regression in mice treated with combinatorial treatment with IL12 and dual-ICI. Immunophenotyping analyses of peritoneal tumor tissue showed clear polarization toward pro-immune function within the TME, with significant increases in the activation of pathways associated with inflammatory responses, particularly IFNγ, IL6/STAT3, and TNF. Notably, a significant downregulation in Wnt/Beta catenin signaling, likely related to the decreased tumor burden, was observed after combinatory treatment with IL12 and dual-ICI. Moreover, lower tumor burden associated with a decrease in gene signatures linked to endothelial cells and mesenchymal stem cells.

In-depth immune profiling confirmed a crucial contribution by the myeloid compartment to the durable responses observed after treatment with IL12 and dual-ICI. Bulk transcriptomic analyses of CD11b+ cells purified from ascites were strikingly similar to those from tumors, revealing a polarization toward pro-immune responses as evidenced by the upregulation of interferon gamma and alpha pathways as wells as IL12, TNF-alpha, and IL-6, among others. The pivotal role of myeloid cells was further confirmed by single-cell transcriptomics comparing peritoneal CD11b+

cells isolated from mice in relapse with those isolated from mice in remission. Our results showed marked differences in the transcriptome of myeloid cells from mice in remission compared to those with progressing tumors, with significant upregulation of molecules known to mediate immune suppression such as S100a8/9/6, MIF, and Arg1 among others in CD11b+ cells obtained from mice in relapse. Our findings underscore the notion that modulating myeloid function can be a potential intervention for enhancing the activity of dual-ICI. Further, these data show that IL12 reduced CCL2/CCR2 axis signaling, which has been shown to promote cancer progression, metastasis, and induces immunosuppressive environment favoring TH2 mediated immune response.[35,36]

Despite its well-known anti-tumor properties, the clinical development of IL12 has been hindered by its potential toxic effects and lack of significant activities when given alone or combined with molecules other than immune checkpoint inhibitors, such as cetuximab or trastuzumab with or without paclitaxel.[37–41] At the dosages outlined in the experiments reported here, triplet therapy was well tolerated by the mice with no evidence of toxicities. Further, all mice reached endpoint due to ascites accumulation (i.e. tumor progression) and none had to be sacrificed due to adverse effects related to any indicated therapy modality. One question that arises from these studies is whether the effect that we noted is dependent on locoregional administration of IL12 since we injected IL12 intraperitoneally to treat intraperitoneal disease. Our preclinical work suggests that the synergistic effect of IL12 and dual-ICI is lost when IL12 is administered subcutaneously [Supplemental Figure S2]. Additional studies are needed to further compare the efficacy and toxicity of systemic versus intraperitoneal locoregional administration of IL12. Lenzi et al. investigated the safety and activity of IL12 when given i.p. to patients with peritoneal carcinomatosis.[35] The authors demonstrated that intraperitoneal IL12 was well tolerated and associated with increased production of IFNγ and CXCL10, decreased tumor expression of vascular endothelial growth factors, and associated with an increased proportion of CD3+ cells relative to CD14+ cells. Our findings support a clinical trial to investigate the efficacy of IL12 combined with dual-ICI for patients with ovarian cancer. This approach is attractive especially with recent advances in novel gene delivery platforms of IL12 like plasmids, mRNA based or viral vectors.[42,43]

Disclosure statement

Funding

References

1. Torre LA, Trabert B, DeSantis CE, Miller KD, Samimi G, Runowicz CD, Gaudet MM, Jemal A, Siegel RL. Ovarian cancer statistics, 2018. CA Cancer J Clin. 2018;68(4):284–296. doi:10.3322/caac.21456.

2. Herzog TJ. The current treatment of recurrent ovarian cancer. Curr Oncol Rep. 2006;8(6):448–454. doi:10.1007/s11912-006-0074-9.

3. Wright AA, Bohlke K, Armstrong DK, Bookman MA, Cliby WA, Coleman RL, Dizon DS, Kash JJ, Meyer LA, Moore KN, et al. Neoadjuvant chemotherapy for newly diagnosed, advanced ovarian cancer: society of Gynecol Oncol and American society of clinical oncology clinical practice guideline. Gynecol Oncol. 2016;143(1):3–15. doi:10.1016/j.ygyno.2016.05.022.

4. Pujade-Lauraine E, Alexandre J. Update of randomized trials in recurrent disease. Ann Oncol. 2011;22(8):viii61–64. doi:10.1093/annonc/mdr518.

5. Pujade-Lauraine E, Hilpert F, Weber B, Reuss A, Poveda A, Kristensen G, Sorio R, Vergote I, Witteveen P, Bamias A, et al. Bevacizumab combined with chemotherapy for platinum-resistant recurrent ovarian cancer: the AURELIA open-label randomized phase III trial. J Clin Oncol. 2014;32(13):1302–1308. doi:10.1200/JCO.2013.51.4489.

6. Mutch DG, Orlando M, Goss T, Teneriello MG, Gordon AN, McMeekin SD, Wang Y, Scribner DR, Marciniack M, Naumann RW, et al. Randomized phase III trial of gemcitabine compared with pegylated liposomal doxorubicin in patients with platinum-resistant ovarian cancer. J Clin Oncol. 2007;25 (19):2811–2818. doi:10.1200/JCO.2006.09.6735.

7. Monk BJ, Herzog TJ, Kaye SB, Krasner CN, Vermorken JB, Muggia FM, Pujade-Lauraine E, Park YC, Parekh TV, Poveda AM. Trabectedin plus pegylated liposomal doxorubicin (PLD) versus PLD in recurrent ovarian cancer: overall survival analysis. Eur J Cancer. 2012;48(15):2361–2368. doi:10.1016/j.ejca.2012.04.001.

8. Meier W, du Bois A, Reuss A, Kuhn W, Olbricht S, Gropp M, Richter B, Lück H-J, Kimmig R, Pfisterer J. Topotecan versus treosulfan, an alkylating agent, in patients with epithelial ovarian cancer and relapse within 12 months following 1st-line platinum/paclitaxel chemotherapy. A prospectively randomized phase III trial by the Arbeitsgemeinschaft gynaekologische onkologie ovarian cancer study group (AGO-OVAR). Gynecol Oncol. 2009;114 (2):199–205. doi:10.1016/j.ygyno.2009.04.026.

9. Buda A, Floriani I, Rossi R, Colombo N, Torri V, Conte PF, Fossati R, Ravaioli A, Mangioni C. Randomised controlled trial comparing single agent paclitaxel vs epidoxorubicin plus paclitaxel in patients with advanced ovarian cancer in early progression after platinum-based chemotherapy: an Italian collaborative study from the Mario Negri institute, Milan, G.O.N.O. (Gruppo oncologico nord ovest) group and I.O.R. (Istituto oncologico romagnolo) group. Br J Cancer. 2004;90(11):2112–2117. doi:10.1038/sj.bjc.6601787.

10. ten Bokkel Huinink W, Gore M, Carmichael J, Gordon A, Malfetano J, Hudson I, Broom C, Scarabelli C, Davidson N, Spanczynski M, et al. Topotecan versus paclitaxel for the treatment of recurrent epithelial ovarian cancer. J Clin Oncol. 1997;15 (6):2183–2193. doi:10.1200/JCO.1997.15.6.2183.

11. Gaillard SL, Secord AA, Monk B. The role of immune checkpoint inhibition in the treatment of ovarian cancer. Gynecol Oncol Res Pract. 2016;3(1):11. doi:10.1186/s40661-016-0033-6.

12. Hamanishi J, Mandai M, Ikeda T, Minami M, Kawaguchi A, Murayama T, Kanai M, Mori Y, Matsumoto S, Chikuma S, et al. Safety and antitumor activity of anti–PD-1 antibody, nivolumab, in patients with platinum-resistant ovarian cancer. J Clin Oncol. 2015;33(34):4015–4022. doi:10.1200/JCO.2015.62.3397.

13. Zamarin D, Burger RA, Sill MW, Powell DJ, Lankes HA, Feldman MD, Zivanovic O, Gunderson C, Ko E, Mathews C, et al. Randomized phase ii trial of nivolumab versus nivolumab and ipilimumab for recurrent or persistent ovarian cancer: an nrg oncology study. J Clin Oncol. 2020;38(16):1814–1823. doi:10.1200/JCO.19.02059.

14. Zhang M, He Y, Sun X, Li Q, Wang W, Zhao A, Di W. A high M1/M2 ratio of tumor-associated macrophages is associated with extended survival in ovarian cancer patients. J Ovarian Res. 2014;7(1):19. doi:10.1186/1757-2215-7-19.

15. Lyons YA, Pradeep S, Wu SY, Haemmerle M, Hansen JM, Wagner MJ, Villar-Prados A, Nagaraja AS, Dood RL, Previs RA, et al. Macrophage depletion through colony stimulating factor 1 receptor pathway blockade overcomes adaptive resistance to anti-VEGF therapy. Oncotarget. 2017;8(57):96496–96505. doi:10.18632/oncotarget.20410.

16. Kryczek I, Wei S, Zhu G, Myers L, Mottram P, Cheng P, Chen L, Coukos G, Zou W. Relationship between B7-H4, regulatory T cells, and patient outcome in human ovarian carcinoma. Cancer Res. 2007;67(18):8900–8905. doi:10.1158/0008-5472.CAN-07-1866.

17. Ni Y, Soliman A, Joehlin-Price A, Abdul-Karim F, Rose PG, Mahdi H. Immune cells and signatures characterize tumor microenvironment and predict outcome in ovarian and endometrial cancers. Immunotherapy. 2021;13(14):1179–1192. doi:10.2217/imt-2021-0052.

18. Ni Y, Soliman A, Joehlin-Price A, Rose PG, Vlad A, Edwards RP, Mahdi H. High TGF-β signature predicts immunotherapy resistance in gynecologic cancer patients treated with immune checkpoint inhibition. NPJ Precis Oncol. 2021;5(1):101. doi:10.1038/s41698-021-00242-8.

19. Tannenbaum CS, Rayman PA, Pavicic PG, Kim JS, Wei W, Polefko A, Wallace W, Rini BI, Morris-Stiff G, et al. Mediators of inflammation-Driven Expansion, Trafficking, and Function of Tumor-Infiltrating MDSCs. Cancer Immunol Res. 2019;7 (10):1687–1699. doi:10.1158/2326-6066.CIR-18-0578.

20. Schmidt CS, Mescher MF. Adjuvant effect of IL12: conversion of peptide antigen administration from tolerizing to immunizing for CD8+ T cells in vivo. J Immunol. 1999;163(5):2561–2567. doi:10.4049/jimmunol.163.5.2561.

21. Salem ML, Kadima AN, Zhou Y, Nguyen CL, Rubinstein MP, Demcheva M, Vournakis JN, Cole DJ, Gillanders WE. Paracrine release of IL-12 stimulates IFN-γ production and dramatically enhances the antigen-specific T cell response after vaccination with a novel peptide-based cancer vaccine. J Immunol. 2004;172 (9):5159–5167. doi:10.4049/jimmunol.172.9.5159.

22. Chang J, Cho J-H, Lee S-W, Choi S-Y, Ha S-J, Sung Y-C. IL12 priming during in vitro antigenic stimulation changes properties of CD8 T cells and increases generation of effector and memory cells. J Immunol. 2004;172(5):2818–2826. doi:10.4049/jimmunol.172.5.2818.

23. Diaz-Montero CM, Ravichandran S, Pavicic PG, Rayman PA, Tannenbaum C, Finke J, Ko JS, Funchain P, Tarhini AA. Low-dose IL-12 preconditions the tumor microenvironment to enhance the efficacy of PD-1 blockade. J Clin Oncol. 2019;37(8_suppl). 20–20. doi:10.1200/JCO.2019.37.8_suppl.20.

24. Watford WT, Moriguchi M, Morinobu A, O'shea JJ. The biology of IL12: coordinating innate and adaptive immune responses. Cytokine Growth Factor Rev. 2003 ;14(5):361–368. doi:10.1016/s1359-.

25. Su W, Ito T, Oyama T, Kitagawa T, Yamori T, Fujiwara H, Matsuda H. The direct effect of IL-12 on tumor cells: iL-12 acts directly on tumor cells to activate NF-κB and enhance IFN-γ-mediated STAT1 phosphorylation. Biochem Biophys Res Commun. 2001;280(2):503–512. doi:10.1006/bbrc.2000.4150.

26. Duraiswamy J, Kaluza KM, Freeman GJ, Coukos G. Dual blockade of PD-1 and CTLA-4 combined with tumor vaccine effectively restores T-cell rejection function in tumors. Cancer Res. 2013;73 (12):3591–3603. doi:10.1158/0008-5472.CAN-12-4100.

27. Dobin A, Gingeras TR. Mapping RNA-seq reads with STAR. Curr Protoc Bioinformatics. 2015;51(1). 14 11–11 14 19 . doi:10.1002/0471250953.bi1114s51.

28. Liao Y, Smyth GK, Shi W. featureCounts: an efficient general purpose program for assigning sequence reads to genomic features. Bioinformatics. 2014;30:923–930. doi:10.1093/bioinformatics/btt656.

29. Love MI, Huber W, Anders S. Moderated estimation of fold change and dispersion for RNA-seq data with DESeq2. Genome Biol. 2014;15(12):550. doi:10.1186/s13059-014-0550-8.

30. Trinchieri G. Interleukin-12 and the regulation of innate resistance and adaptive immunity. Nat Rev Immunol. 2003;3(2):133–146. doi:10.1038/nri1001.

31. Diaz-Montero CM, El Naggar S, Al Khami A, El Naggar R, Montero AJ, Cole DJ, Salem ML. Priming of naive CD8+ T cells in the presence of IL12 selectively enhances the survival of CD8 +CD62Lhi cells and results in superior anti-tumor activity in a tolerogenic murine model. Cancer Immunol Immunother. 2008;57(4):563–572. doi:10.1007/s00262-007-0394-0.

32. Grasso CS, Tsoi J, Onyshchenko M, Abril-Rodriguez G, Ross-Macdonald P, Wind-Rotolo M, Champhekar A, Medina E, Torrejon DY, Shin DS, et al. Conserved interferon-γ signaling drives clinical response to immune checkpoint blockade therapy in melanoma. Cancer Cell. 2020;38(4):500–515 e503. doi:10.1016/j.ccell.2020.08.005.

33. Roby KF, Taylor CC, Sweetwood JP, Cheng Y, Pace JL, Tawfik O, Persons DL, Smith PG, Terranova PF. Development of a syngeneic mouse model for events related to ovarian cancer. Carcinogenesis. 2000;21(4):585–591. doi:10.1093/carcin/21.4.585.

34. Okla K, Czerwonka A, Wawruszak A, Bobiński M, Bilska M, Tarkowski R, Bednarek W, Wertel I, Kotarski J. Clinical relevance and immunosuppressive pattern of circulating and infiltrating subsets of myeloid-derived suppressor cells (MDSC) in epithelial ovarian cancer. Front Immunol. 2019;10:691. doi:10.3389/fimmu.2019.00691.

35. Furukawa S, Soeda SH, Kiko Y, Suzuki O, Hashimoto Y, Watanabe T, Nishiyama H, Tasaki K, Hojo H, Abe M, Fujimori K. et al. MCP-1 promotes invasion and adhesion of human ovarian cancer cell. Anti-Cancer Res 2013;3(11):4785–4790.

36. Mandal PK, Biswas S, Mandal G, Purohit S, Gupta A, Majumdar (Giri) A, Roy Chowdhury S, Bhattacharyya A. CCL2 conditionally determines CCL22-dependent Th2-accumulation during TGF-β-induced breast cancer progression. Immunobiology. 2018;223(2):151–161. doi:10.1016/j.imbio.2017.10.031.

37. Lenzi R, Rosenblum M, Verschraegen C, Kudelka AP, Kavanagh JJ, Hicks ME, Lang EA, Nash MA, Levy LB, Garcia ME, et al. Phase I study of intraperitoneal recombinant human interleukin 12 in patients with Müllerian carcinoma, gastrointestinal primary malignancies, and mesothelioma. Clin Cancer Res. 2002;8(12):3686–3695.

38. Lenzi R, Edwards R, June C, Seiden MV, Garcia ME, Rosenblum M, Freedman RS. Phase II study of intraperitoneal recombinant interleukin-12 (rhIL-12) in patients with peritoneal carcinomatosis (residual disease < 1=cm) associated with ovarian cancer or primary peritoneal carcinoma. J Transl Med. 2007;5(1):66. doi:10.1186/1479-5876-5-66.

39. Bekaii-Saab TS, Roda JM, Guenterberg KD, Ramaswamy B, Young DC, Ferketich AK, Lamb TA, Grever MR, Shapiro CL, Carson WE. A phase I trial of paclitaxel and trastuzumab in combination with interleukin-12 in patients with HER2/neu-expressing malignancies. Mol Cancer Ther. 2009 ;8(11):2983–2991. doi:10.1158/1535-.

40. Parihar R, Nadella P, Lewis A, Jensen R, De Hoff C, Dierksheide JE, VanBuskirk AM, Magro CM, Young DC, Shapiro CL, et al. A phase I study of interleukin 12 with trastuzumab in patients with human epidermal growth factor receptor-2-overexpressing malignancies: analysis of sustained interferon gamma production in a subset of patients. Clin Cancer Res. 2004;10(15):5027–5037. doi:10.1158/1078-0432.CCR-04-0265.

41. McMichael EL, Benner B, Atwal LS, Courtney NB, Mo X, Davis ME, Campbell AR, Duggan MC, Williams K, Martin K, et al. A phase I/II trial of cetuximab in combination with interleukin-12 administered to patients with unresectable primary or recurrent head and neck squamous cell carcinoma. Clin Cancer Res. 2019;25(16):4955–4965. doi:10.1158/1078-0432.CCR-18-2108.

42. Thaker PH, Bradley WH, Leath CA, Gunderson Jackson C, Borys N, Anwer K, Musso L, Matsuzaki J, Bshara W, et al. GEN-1 in combination with neoadjuvant chemotherapy for patients with advanced epithelial ovarian cancer: a phase I dose-escalation study. Clin Cancer Res. 2021;27(20):5536–5545. doi:10.1158/1078-0432.CCR-21-0360.

43. Cirella A, Luri-Rey C, Di Trani CA, Teijeira A, Olivera I, Bolaños E, Castañón E, Palencia B, Brocco D, et al. Novel strategies exploiting interleukin-12 in cancer immunotherapy. Pharmacol Ther. 2022;239:108–189. doi:10.1016/j.pharmthera.2022.108189.